Journal Pre-proof
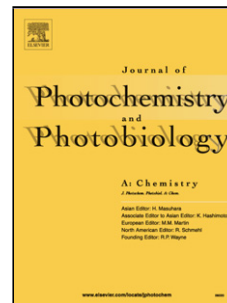
Long-range photoinduced charge separation in tröger bases D/A dyads

Diego Dusso, Priscila A. Lanza, Hernán A. Montejano, Cristina L. Ramírez, Alejandro R. Parise, D.Mariano A. Vera, E. Laura Moyano, Carlos A. Chesta

Please cite this article as: { doi: https://doi.org/

Long-range photoinduced charge separation in Tröger bases D/A dyads

Diego Dusso [a], Priscila A. Lanza [b], Hernán A. Montejano [c], Cristina. L. Ramírez [d], Alejandro R. Parise [d], D. Mariano A. Vera [b]*, E. Laura Moyano [a]**, and Carlos A. Chesta. [c]***

a INFIQC. Departamento de Química Orgánica. Facultad de Ciencias Químicas. Universidad Nacional de Córdoba, Córdoba, Argentina.
b QUIAMM-INBIOTEC. Departamento de Química. Facultad de Ciencias Exactas y Naturales. Universidad Nacional de Mar del Plata. Mar del Plata. Argentina.
c IITEMA. Departamento de Química, Facultad de Ciencias Exactas y Naturales, Universidad Nacional de Río Cuarto, Argentina.
d Departamento de Química. Facultad de Ciencias Exactas y Naturales. Universidad Nacional de Mar del Plata. Mar del Plata. Argentina.
* E-mail: dmavera@yahoo.com
** E-mail: lauramoy@fcq.unc.edu.ar
*** E-mail: cchesta@exa.unrc.edu.ar

Graphical abstract

Highlights for: Long-range photoinduced charge separation in Tröger bases D/A dyads

- Two novel series of D/A Tröger base (TB) dyads were synthesized and characterized
- All TB dyads show large degrees of charge separation (CT) in their excited states

- Depending of the D/A redox gap, CT can involve one or both N of the TB diazocine ring
- For larger D/A gaps, TB dyads excited state dipole moments riche values ~24-35 D
- TB diazocine ring can behave as a π bridge

Abstract

Tröger´s base (and its derivatives) are compounds comprised of two aromatic (or polyaromatic) rings bridged by a diazocine aliphatic cycle. We report herein the photophysical properties of two series of novel Tröger´s bases (TB) asymmetrically substituted by electron donor (D) and electron acceptor (A) substituents. In TB series **3**, a carbonitrile group (A=CN) lies at the position 2 of the heterocycle, while position 8 is occupied by a series of D with increasing reductant capacity: H (**3a**), CH_3 (**3b**), OCH_3 (**3c**) or $N(CH_3)_2$ (**3d**). A novel TB series (**5a**-**5d**) which comprise the same D, but a 2,2-dicyanovinyl group (A=$CHC(CN)_2$) as electron acceptor, was synthesized and fully characterized. TB absorption (ν_A^{max}) and emission energies (ν_F^{max}), fluorescence quantum yields (Φ_F) and emission lifetimes (τ_F) were determined in a series of aprotic solvents covering a wide range of medium polarity (ε~2-38). ν_F^{max}, Φ_F and τ_F largely depend on the polarity of the medium and the nature of D/A pair. From the solvatochromic study on ν_F^{max}, it is concluded that upon excitation TB´s develop large degrees of charge separation (CT). Photophysically, **3a-3c** resembles 4-(*N,N*-dimethylamino)benzonitrile derivatives showing internal CT state dipole moments (μ_1^*) of ~ 15-17 D. For **3d** and the entire series **5**, CT occurs throughout the diazocine ring giving rise to giant μ_1^* (> 25 D). This is indeed an unusual result, because it strongly suggests that the aliphatic diazocine ring can couple the D/A redox centers as a π bridge would do.

Keywords: Tröger´s base, electron donor/acceptor dyad, charge transfer, giant dipole moment, photophysics

Introduction

Tröger (TB) bases and its derivatives are V-shaped, rigid and chiral compounds that have attracted attention for decades due to their multiple applications, [1] such as

fluorescent probes [2], synthetic receptors, [3-4] supramolecular chemistry, [5] and catalysts. [6] TB have been also explored as promising materials for the fabrication of OLED [7], optoelectronic devices [8] and for non-linear optical applications. [9] We report herein the synthesis and photophysical characterization of novel TB asymmetrically substituted by the D/A groups (Figure 1) to better understand how these substituents modify the absorption and emission properties of these synthetic dyes, aiming to improve their structures for optoelectronic applications, among others.
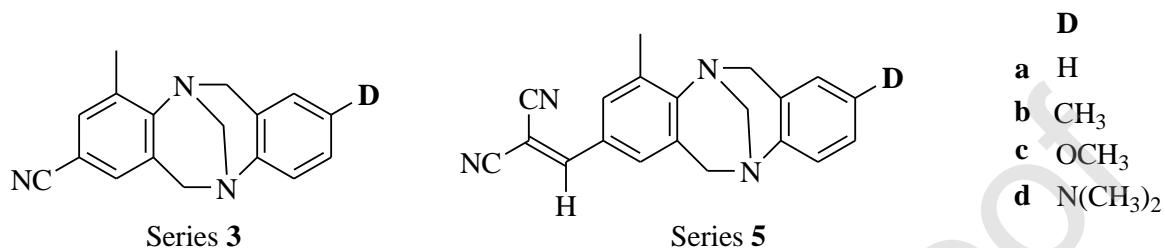

	D
a	H
b	CH_3
c	OCH_3
d	$N(CH_3)_2$

Figure 1: Molecular structure of TBs series **3** and **5**

Materials and methods

TB series **3** and **5** were prepared following synthetic procedures recently developed. [10] Experimental details of the synthesis as well as, of the experiments performed to characterize the photophysics of the TBs are provided in the ESI.

Results and discussion

The most relevant information on the absorption properties of TB is summarized in Table 1-ESI. Figure 2a shows the absorption spectra obtained for series **3** in cyclohexane. Compounds **3a-3b** exhibit two main absorption bands at ~250 and ~290 nm. Absorption of **3c** is slightly red shifted and shows a moderate increase of the (maxima) molar absorption coefficients. For **3d**, D = $N(CH_3)_2$, the absorption spectrum is remarkably different. In all solvents studied, the spectra of **3d** are clearly shifted to lower energies and a new weak transition appears at ~370 nm. Interestingly, the absorption spectra of TB series **3** are practically insensitive to the polarity of the medium (see Table 1-ESI). Substitution of the CN group by a dicyanovinyl group (series **5**) leads to a large shift of the absorption to lower energies. Absorption spectra obtained for series **5** in cyclohexane are collected in Figure 2b. TBs **5a-5c** show two bands between 300-450 nm, which apparently shift to the red and decrease in intensity as the reducing power of D increases. Again, amine derivative **5d** behaves somehow

4

differently. Both main absorption bands shift hipsochromically and the spectrum widen to >450 nm.
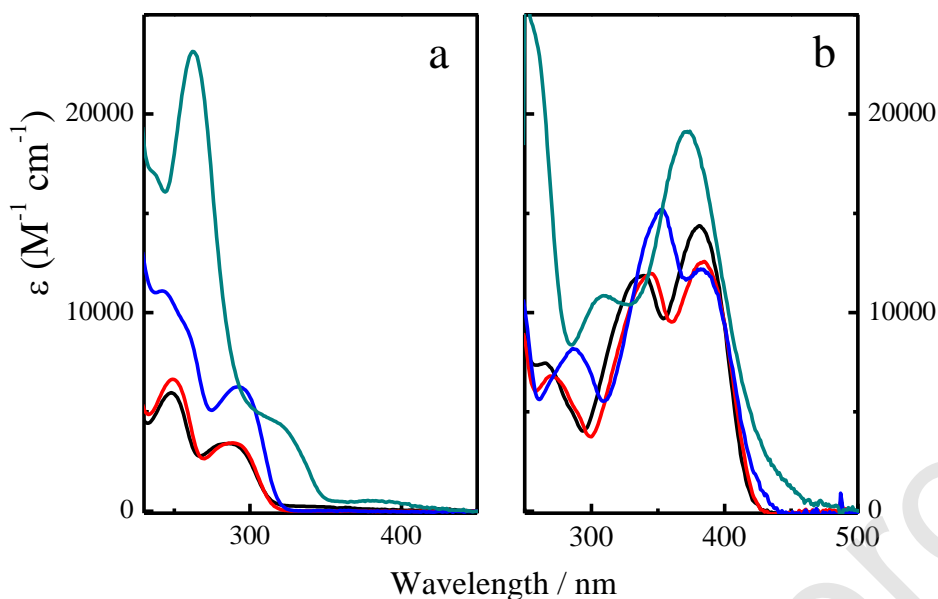

Figure 2. Absorption spectra of TB series **3** (panel a) and **5** (panel b) recorded in cyclohexane at 298 K: **a** (black), **b** (red), **c** (blue) and **d** (green).

Although TBs compounds show significant emission in the solid state, [11] they are scarcely fluorescent in fluid media. For TB series **3**, Φ_F ranges between ~0.07-0.001, while for series **5** Φ_F values go between ~0.008-0. In general, Φ_F decreases with increasing solvent polarity and increasing D-A redox gap. Within a TB series the emission efficiency follows the trend: **a~ b** > **c** > **d**; and if TB series are compared, always TB from series **3** emits more than the corresponding TB from series **5** (Table 1-ESI). These observations are illustrated in Figures 3a and 3b. Figure 3a shows the solvent effect on the (normalized) emission spectrum of **3a**. As shown, **3a** fluorescence progressively shifts to lower energies as the polarity of the solvent increase. This result suggests that the excited state of **3a** is largely polar. It is interesting to note that structurally, **3a** is closely related to 4-(*N,N*-dimethylamino)benzonitrile (DMABN). DMABN has been extensively studied due to its unusual dual fluorescence, which arises from local excited (LE) and twisted internal charge transfer (TICT) states. [12] However, none of the TB studied here show dual emission. This is probably due to the TB´s molecular rigidity that makes free rotation of N (in *p*- position to the CN group) impossible. In fact, the photophysical behaviour of **3a** is quite similar to the observed

for 6-cyanobenzquinuclidine (CBQ) [13], a rigid derivative of DMABN. In CBQ and other related compounds (see Scheme 1-ESI), the N lone pair is nearly perpendicular to the π system (as in TB) and therefore, emission occurs almost exclusively from the TICT state. In addition, Φ_F (<0.08) and τ_F (~1.09 ns) values determined for CBQ in cyclohexane and its (TICS) excited state dipole moment (~13-15 D) are in very good agreement with those calculated for **3a** (*vide infra*). Figure 3b shows the normalized fluorescence spectra of series **5** in cyclohexane. As shown, TB´s emission increasingly shifts to lower energy with increasing D reducing capacity. Also Φ_F decreases markedly; for **5d** the emission efficiency is so low (~10^{-3}) that Raman dispersion of the solvent can be observed.
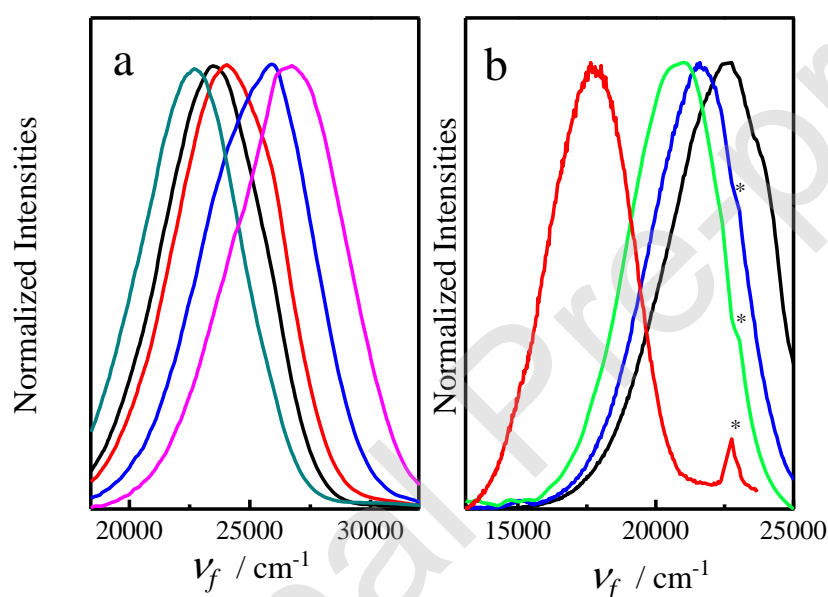

Figure 3. a) Emission spectra of **3a** recorded in aprotic solvents at 298 K: cyclohexane (magenta), butyl ether (blue), ethyl acetate (red), dichloromethane (black) and acetonitrile (dark green). b) Emission spectra of TB series **5** recorded in cyclohexane at 298 K: **5a** (black), **5b** (blue), **5c** (green) and **5d** (red). Peaks denoted by * corresponds to the Raman dispersion of the solvents. Emission spectra were obtained by 280 nm excitation for series **3** and 380 nm for series **5**.

Table 1-ESI also collects τ_F values measured for those TB/solvent systems with Φ_F larger than ~10^{-3}. In most cases, emission profiles could be fitted to a monoexponential decay function. Exceptions are **3d**, **5c** and **5d** in cyclohexane and **3d** in butyl ether,

which apparently decays biexponentially. Unfortunately, the low Φ_F observed for these TBs made technically impossible to perform time resolved emission spectra (TRES) experiments aimed to unravel this behaviour. From the analysis of data in Table 1-ESI, clear trends of τ_F, the radiative ($k_R = \Phi_F / \tau_F$) and nonradiative ($k_{NR} = 1/\tau_F - k_R$) rate constants with solvent polarity can be found. For both TB series, τ_F increases with increasing solvent polarity while k_R and k_{NR} decrease. This behaviour is typical of excited states exhibiting large degrees of CT (inter and intramolecular exciplexes, TICS, etc.). Laser flash photolysis experiments conducted for **3a** and **3d** in cyclohexane and **3a** in acetonitrile did not show absorptions due to the formation of triplet excited species in the 0.5-200 μs time scale. From these results it is concluded that TBs singlet excited states decay mainly *via* internal conversion. The low Φ_F observed for TB series **5** is due to the efficient nonradiative deactivation processes that affect these bases. Interestingly, 2-[4-(dimethylamino)benzylidene]) malononitrile (structurally related to **5a,** see Scheme 2-ESI) shows a similar behaviour. [14] The large k_{NR} observed for these compounds is apparently due to the dicyanovinyl group which provides extra (rotational) energy acceptor states that favour the horizontal radiationless transition. In Figure 4, the experimental values of ν_F^{max} are plotted according to Lippert solvatochromic model. [15] For pull-push chromophores (*vide infra*), ν_F^{max} solvent dependence is conveniently interpreted according to:

$$\nu_F^{max} \cong \left[\mu_1^* \left(\mu_0^* - \mu_1^* \right) / hca^3 \right] f\left(\varepsilon, n^2 \right) + C_F , \tag{1}$$

where, μ_1^* and μ_0^* are the (vector) dipole moments of the relaxed singlet excited (S_1^*) and unrelaxed ground state (S_0^*), respectively, a represents radius of the Onsager's solvent cavity, C_F is a constant for a given fluorophore and $f\left(\varepsilon, n^2 \right)$ is the Lippert parameter (see ESI). Therefore, from the slopes of the plots in Figure 4 raw estimates of μ_1^* cane obtained if a and μ_0^* are known. As shown in Figure 4, the slopes of the Lippert plots for **3a-3c** are similar (Table 2-ESI). Using for a and μ_0^* (considered parallel to μ_1^*) the same values assumed for CBQ;[7] *i.e.*: ~0.4-0.5 nm and ~4.05 D, respectively, a $\mu_1^* \sim$ 15-17 D is calculated for **3a-3c**. Since this value agrees very well with that reported for CBQ, it seems reasonable to propose for **3a-3c** that CT in the

7

excited state only involves the first N of the diazocine bridge; this is, the one which is in the same phenyl ring as the CN group. Interestingly, for TB with larger D/A redox gaps (**3d** and **5a-5c)** slopes are also similar but considerably larger as compared with **3a-3c**. Hence, taking into account that in the excited states of **3a-3c** (as well as in CBQ, DMABN, etc.) nearly full charge separation is already achieved, (*i.e.*: $\mu_1^* \propto r|q|$ with $|q| \sim 1$ electronic charge in atomic units), the only way to explain the increased Lippert plots slopes observed for **3d** and **5a-5c** is that separation (*r*) between opposite charge densities grows considerably. Accordingly, we propose that excitation of **3d** and **5a-5c** leads to CT states that extend throughout the entire molecular structures and involves both TB´s phenyl rings. Note that although a crude estimate of a for these systems would be feasible using molecular models, CT occurring between the two TB aromatic rings would make μ_0^* and μ_1^* not parallel precluding any realistic estimation of $\mu_1^*\left(\mu_0^* - \mu_1^*\right)$. Still, preliminary TDDFT quantum mechanical calculations support this interpretation and predict for **3a-3c** μ_1^* in the order of 15-17 D and values of 24-35 D for **3d** and **5a-5c.** For instance, Figure 5 shows the calculated transition density for S_1^*, μ_0^* and μ_1^* for **5c** in ethyl acetate. For details see ESI and Table 4-ESI. It is interesting to remark that these TBs both rings containing D and A centers are connected through an aliphatic bridge, thus turning this long-range CT unusual *per se.* However, an effective connection between the D/A centers bridge by the diazocine moiety was not completely unexpected. Indeed, such unusual electronic coupling was already observed for symmetrical TBs upon dark one-electron oxidation. [3] Detailed ab initio computational calculations are currently being attempted to fully explain this unusual D/A coupling, results that will be reported shortly.
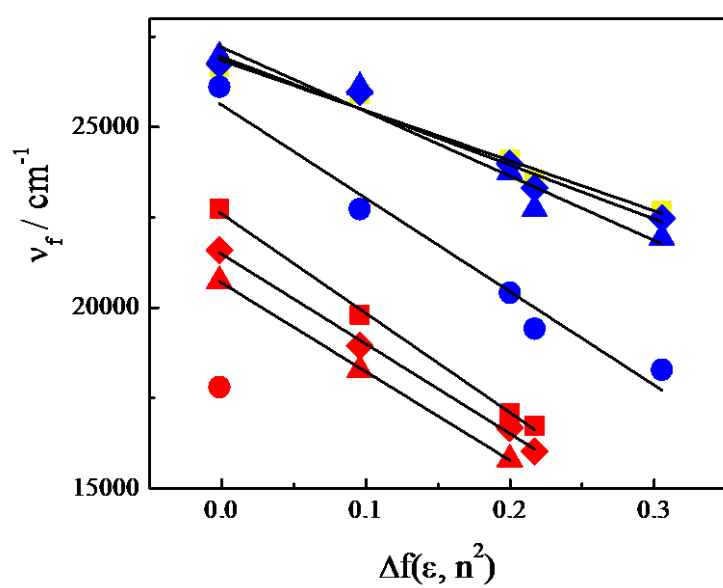
Figure 4: Lippert plots for TB series **3** (blue) and **5** (red): **a** (squares), **b** (diamonds), **c** (triangles) and **d** (circles).
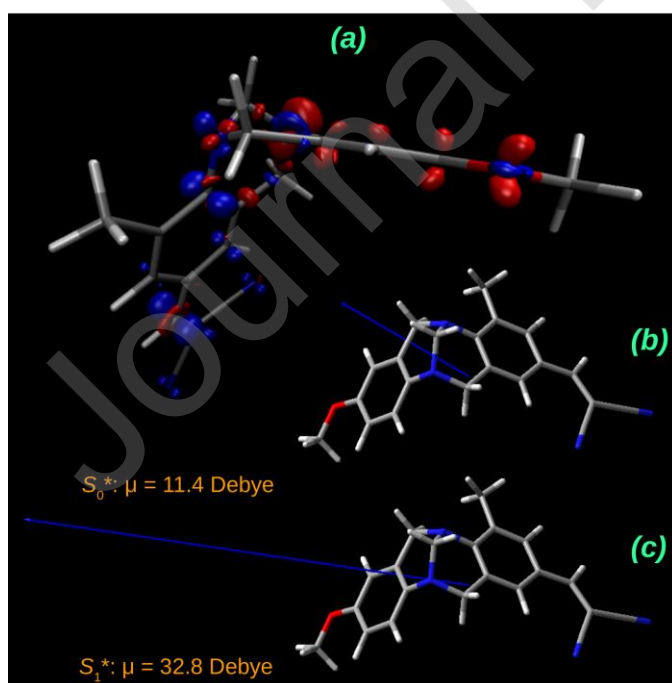
Figure 5: (a) Calculated transition density for the emitting CT state (S_1^*) of **5c** in ethyl acetate as model solvent. The isosurface was obtained as the difference between the total electronic density of the upper and lower states. It resembles the difference between the main donor and acceptor orbitals (in this case HOMO and LUMO, see also ESI Figure 1-ESI). Isosurfaces scales corresponds to red = - 0.008 e (accounting for all donor or starting orbitals) and blue = + 0.008 e (acceptor or final orbitals). The resulting marked CT from the anisyl to dicianovinyl moieties explains the huge increase in the dipole moment of the S_1^* with respect to S_0^*. (b-c) Calculated dipole moment vectors for the S_0^* and S_1^* states, respectively (scale factor of 0.51 for both).

Conclusions

All TBs studied show clear pull-push behaviour. TBs with smaller D/A redox gaps separates charge from the diazocine N to the CN acceptor group and behave similarly to rigid DMABN derivatives. However, for the TBs with large redox gaps, CT can involve the whole molecule, from edge to edge, creating very large excited state dipole moments. In these cases, TBs behave as compounds where D and A edges are electronically coupled through a π bridge. This feature, combined with its molecular shape and rigidity, will allow the design of new TB structures with improved properties for various applications, particularly as optoelectronics materials.

Competing interests
The authors declare no competing financial interest.

10

References

[1] Synthesis and applications of TBs has been extensively reviewed, see for instance: a) Rúnarsson, Ö. V., Artacho, J., Wärnmark, K. The 125th anniversary of the Tröger's base molecule: Synthesis and applications of Tröger's base analogues. *European Journal of Organic Chemistry* **2012**, (36), 7015-7041, b) Dolenský B, Elguero J., Král V., Pardo C, Valik M. Current Tröger's base chemistry. *Advances in Heterocyclic Chemistry* **2007**; 93:1-56, c) Valik, M., Strongin, R. M., Král, V. Tröger's Base Derivatives—New Life for Old Compounds. *Supramolecular Chemistry* **2005**, *17*(5), 347-367.

[2] Calatrava-Pérez, E., Delente, J. M., Shanmugaraju, S., Hawes, C. S., Williams, C. D., Gunnlaugsson, T., Scanlan, E. M.. Glycosylated naphthalimides and naphthalimide Tröger's bases as fluorescent aggregation probes for Con A. *Organic & biomolecular chemistry*, **2019**, *17*(8), 2116-2125.

[3] Hansson, A. P., Norrby, P. O., & Wärnmark, K. A bis (crown-ether) analogue of Tröger's base: Recognition of achiral and chiral primary bisammonium salts. *Tetrahedron letters*, **1998**, *39*(25), 4565-4568.

[4] Baldeyrou, B., Tardy, C., Bailly, C., Colson, P., Houssier, C., Charmantray, F., & Demeunynck, M. Synthesis and DNA interaction of a mixed proflavine–phenanthroline Tröger base. *European journal of medicinal chemistry*, **2002**, *37*(4), 315-322.

[5] Shanmugaraju, S., Dabadie, C., Byrne, K., Savyasachi, A. J., Umadevi, D., Schmitt, W., Gunnlaugsson, T. A supramolecular Tröger's base derived coordination zinc polymer for fluorescent sensing of phenolic-nitroaromatic explosives in water. *Chemical science*, **2017**, *8*(2), 1535-1546.

[6] Goldberg, Y., & Alper, H. Transition metal complexes of Tröger's base and their catalytic activity for the hydrosilylation of alkynes. *Tetrahedron letters*, **1995**, *36*(3), 369-372.

[7] a) Yuan, C., Xin, Q., Liu, H., Wang, L., Jiang, M., & Tao, X. *Science China Chemistry*, **2011**; *54*(4), 587-595; b) Yuan CX, Tao XT, Ren Y, Li Y, Yang JX, Yu W-T, Wang L, Jiang MH. Synthesis, structure, and aggregation-induced emission of a novel lambda (Λ)-shaped pyridinium salt based on Tröger´s base. *J. Phys. Chem. C* **2007**; *111*:12811-12816.; c) Xin Q, Tao XT, Wang FZ, Sun JL, Zou DC, Wanga FJ, Liu HJ, Liu Z, Jiang MH. *Organic Electronics* **2008**; *9*:1076–1086.

[8] a) Ramirez CL, Procaccini R, Chesta CA, Parise AR, Vera DMA. Selective charge transfer in donor/acceptor systems bridged by Tröger base derivatives. *Organic*

Electronics **2013**; *14*:2564-2572; b) C. L. Ramirez, L. Trupp, A. Bruttomesso, V. T. Amorebieta, D. M. A. Vera, A. R. Parise, Charge transfer properties of Troger base derivatives, *Phys. Chem. Chem. Phys*, **2011,** *13***,** 20076-20080

[9] Sergeyev S, Didier D, Boitsov V, Teshome A, Asselberghs I, Clays K, Vande Velde MLC, Plaquet A, Champagne B. Symmetrical and Nonsymmetrical Chromophores with Trögers Base Skeleton: Chiroptical, Linear, and Quadratic Nonlinear Optical Properties— A Joint Theoretical and Experimental Study. *Chemistry–A European Journal* **2010**; *16*:8181-8190.

[10] Dusso D, Ramirez C, Parise A, Lanza P, Vera DM, Chesta C, Moyano EL, Akhmedov NG. Synthesis of new cyano-substituted analogues of Tröger's bases from bromo-derivatives. A stereochemical dependence of long-range ($^{n}J_{HH}$, n = 4, 5, and 6) proton-proton and proton-carbon ($^{n}J_{CH}$, n = 1, 2, 3, 4, and 5) coupling constants of these compounds. *Magnetic Resonance in Chemistry*. **2019**; 57:423-454.

[11] Chu, Y. H., Wan, Y., Liu, Z. T., Han, X. E., Wu, H.. Synthesis and aggregation-induced emission properties of dicyanovinyl substituted Tröger's bases. *Tetrahedron letters* **2015**, *56*(50), 7046-7052.

[12] Lipiński J, Chojnacki H, Grabowski ZR, Rotkiewicz K. Theoretical model for the double fluorescence of *p*-cyano-*N,N*-dimethylaniline in polar solvents. *Chemical physics letters* **1980**; 70(3): 449-453.

[13] a) Rotkiewicz K. Intramolecular electron-transfer excited state in 6-cyanobenzquinuclidine. *Chemical Physics Letters* **1980**; *70*(3):444-448; b) Köhler, G., Rechthaler, K., Grabner, G., Luboradzki, R., Suwińska, K., Rotkiewicz, K. (). Structure of cage amines as models for twisted intramolecular charge-transfer states. *The Journal of Physical Chemistry A*, **1997**; 101(45), 8518-8525.

[14] Jin H, Liang M, Arzhantsev S, Li X, Maroncelli M. Photophysical characterization of benzylidene malononitriles as probes of solvent friction. *The Journal of Physical Chemistry B* **2010**; 114(22): 7565-7578.

[15] Jara GE, Solis CA, Gsponer NS, Torres JJ, Glusko CA, Previtali CM, Pierini AB, Vera DMA, Chesta CA, Montejano HA. An experimental and TD-DFT theoretical study on the photophysical properties of Methylene Violet Bernthsen. *Dyes and Pigments* **2015**; 112:341-351 and references therein.

References